ON THE OPTICAL–X-RAY CORRELATION FROM OUTBURST TO QUIESCENCE IN LOW-MASS X-RAY BINARIES: THE REPRESENTATIVE CASES OF V404 CYG AND CEN X-4

F. Bernardini[1], D. M. Russell[1], K. I. I. Kolojonen[1], L. Stella[2], R. I. Hynes[3], AND S. Corbel[4]

[1] New York University Abu Dhabi, P.O. Box 129188, Abu Dhabi, United Arab Emirates; bernardini@nyu.edu
[2] INAF—Osservatorio astronomico di Roma, Via Frascati 44, Monteporzio I-00040, Catone (Roma), Italy
[3] Department of Physics and Astronomy, Louisiana State University, 202 Nicholson Hall, Tower Drive, Baton Rouge, LA 70803, USA
[4] Laboratoire AIM (CEA/IRFU—CNRS/INSU—Université Paris Diderot), CEA DSM/IRFU/SAp, F-91191 Gif-sur-Yvette, France

ABSTRACT

Low-mass X-ray binaries (LMXBs) show evidence of a global correlation of debated origin between X-ray and optical luminosity. We study for the first time this correlation in two transient LMXBs, the black hole (BH) V404 Cyg and the neutron star Cen X-4, over six orders of magnitude in X-ray luminosity, from outburst to quiescence. After subtracting the contribution from the companion star, the Cen X-4 data can be described by a single power-law correlation of the form $L_{\rm opt} \propto L_{\rm X}^{0.44}$, consistent with disk reprocessing. We find a similar correlation slope for V404 Cyg in quiescence (0.46) and a steeper one (0.56) in the outburst hard state of 1989. However, V404 Cyg is about 160–280 times optically brighter, at a given 3–9 keV X-ray luminosity, compared to Cen X-4. This ratio is a factor of 10 smaller in quiescence, where the normalization of the V404 Cyg correlation also changes. Once the bolometric X-ray emission is considered and the known main differences between V404 Cyg and Cen X-4 are taken into account (a larger compact object mass, accretion disk size, and the presence of a strong jet contribution in the hard state for the BH system), the two systems lie on the same correlation. In V404 Cyg, the jet dominates spectrally at optical–infrared frequencies during the hard state but makes a negligible contribution in quiescence, which may account for the change in its correlation slope and normalization. These results provide a benchmark to compare with data from the 2015 outburst of V404 Cyg and, potentially, other transient LMXBs as well.

Key words: accretion, accretion disks – stars: black holes – stars: individual (V404 Cyg, Cen X-4) – stars: neutron – X-rays: binaries

1. INTRODUCTION

Low-mass X-ray binaries (LMXBs) are binary systems in which a compact object, a black hole (BH), or a neutron star (NS) accretes matter from a low-mass companion. Many LMXBs are transient and alternate long periods of quiescence, lasting up to many decades, where the X-ray luminosity is low (of the order of a few times 10^{30} to a few times 10^{33} erg s^{-1}), with shorter periods of activity called outbursts, lasting weeks to years, where the X-ray emission is much higher (up to 10^{37}–10^{38} erg s^{-1}) and may approach the Eddington limit. The characteristics of the quiescence/outburst cycle are broadly explained by the disk instability model (DIM; see, e.g., Cannizzo 1993; Lasota 2001). Matter from the companion star accumulates in the accretion disk during quiescence, when the X-ray emission is low; then, during outburst, it is accreted toward the compact object, and the X-ray luminosity increases by orders of magnitude.

At the beginning and at the end of an outburst, LMXBs are found in the so-called low-hard state (see, e.g., Belloni 2010, for a review on XB spectral states), where the X-ray spectrum is dominated by a nonthermal power law. The origin of this spectral component, which extends up to the hard X-ray frequencies, is still unclear. It is commonly accepted that it is produced in a hot corona that surrounds the compact object and Compton upscatters the seed photons emitted by the accretion disk (in the UV and soft X-ray frequencies), or at the base of a compact jet (see Markoff et al. 2005, and references therein).

In BH X-ray binaries (BHXBs) the quiescent and low-hard states share similar properties. For example, a steady compact jet is detected in both states and produces a flat or slightly inverted radio spectrum. Quiescence has been long seen as a low-luminosity version of the hard state. However, recent observations suggest that they could be two distinct states. For example, in some cases the BHXB spectra soften toward quiescence, as a result of the steepening of the X-ray power law (Plotkin et al. 2015).

The emission processes in the optical–infrared (OIR) and UV bands are still poorly known for LMXBs. Several different, and possibly competing, emission mechanisms are expected to contribute at the relevant frequencies, depending on the source type and spectral state. The spectral energy distribution (SED) of quiescent LMXBs is characterized by an excess in the OIR (up to the UV band), with respect to the emission of the companion star alone. This excess is expected to trace the accretion flow; however, the physical mechanisms producing it and the exact location in the binary where these processes take place are still debated. Optical studies suggest that the excess could be intrinsic emission from a hot inner region of the disk (Hynes & Robinson 2012), perhaps due to magnetic reconnections (see, e.g., Hynes et al. 2003; Zurita et al. 2003), or emission produced by the gravitational energy released by matter close to the circularization radius in BH systems, and by the interaction of the pulsar relativistic wind and the inflowing matter in NS systems (Campana & Stella 2000). It could also be produced by X-ray reprocessing from an irradiated disk (Bernardini et al. 2013; Cackett et al. 2013) or by compact jets whose emission may also extend up to X-ray and γ-ray energies (see, e.g., Markoff et al. 2005; Nowak et al. 2011; Pe'er & Markoff 2012; Zdziarski et al. 2014).

In transient LMXBs a fruitful method to understand the origin of the emission at low frequencies (radio, OIR, and UV) is to study its correlation with the X-ray emission using

simultaneous observations. When comparing radio and X-ray fluxes, a tight power-law correlation was found ($L_R \propto L_X^{0.6-0.7}$; Corbel et al. 2003, 2008; Gallo et al. 2003, 2006), suggesting a strong link between radio and X-ray emission, and that the X-ray band could be dominated by synchrotron emission from the jet (Markoff et al. 2001, 2003). Later on, a number of outliers departing from the correlation were identified, showing that two independent tracks are present (with slope 0.68 and 0.98; Gallo et al. 2012). The origin of these two tracks is still unclear. A similar study was also conducted on NS LMXBs, and a radio–X-ray correlation was found with a steeper slope of 1.4. NSs are fainter in the radio, for a given X-ray luminosity, compared to BHs (Migliari & Fender 2006).

The spectral signature of a synchrotron-emitting jet has been found in several BHXBs during quiescence (including V404 Cyg), at either radio (Gallo et al. 2005, 2006, 2014; Plotkin et al. 2015) or infrared (Gallo et al. 2007; Gelino et al. 2010; Shahbaz et al. 2013) frequencies. Although infrared excesses in the broadband spectra have also been interpreted as due to dust or circumbinary emission (Muno & Mauerhan 2006), in some cases at least this emission is variable, implying a synchrotron origin (Russell et al. 2013; Shahbaz et al. 2013). NSXB jets, if they exist in quiescence, are expected to be much fainter than BHXB jets (Migliari & Fender 2006) and have only been reported in one quiescent system (Baglio et al. 2013) and one source at a low (but not quiescent) luminosity (Deller et al. 2014).

OIR and X-ray studies, including data from the NS system Cen X-4 and the BH system V404 Cyg, have shown that there exists a global correlation with a slope of 0.6 ± 0.1 in NSXBs in outburst and BHXBs in the outburst hard state, also extending to quiescence (Russell et al. 2006, 2007). This suggests that synchrotron emission from the jet can play an important role also at IR and optical frequencies. However, X-ray reprocessing from the disk (see also van Paradijs & McClintock 1994) and intrinsic emission from a viscously heated disk can also account for the observed correlation, depending on frequency band (optical, NIR) and source type. The exact contribution from different emission processes depends on a number of parameters, including the disk size and the shape of the jet spectrum (Russell et al. 2006).

In the case of the BH system GX 339-4 in the hard state the optical emission shows a power-law correlation with a slope of 0.44 ± 0.01 (Coriat et al. 2009), while the NIR emission correlates with the X-ray following a broken power-law correlation. These authors conclude that the NIR is jet dominated, while in the optical another component dominates, probably reprocessing in the disk (see also Homan et al. 2005), and the jet contributes about 40%. In BH system XTE J1817-330 the near-UV flux and the hard X-ray flux show a power-law correlation with index 0.5 in the decline from its 2006 outburst up to the return to the low/hard state, suggesting that X-ray reprocessing is the dominating mechanism at near-UV frequency (Rykoff et al. 2007).

More recent studies show that irradiation and reprocessing play an important role also in quiescence. In the case of the NS Cen X-4, when strictly simultaneous optical/UV and X-ray data were used, a short-timescale ($\lesssim$days) correlation was found. The shape of this correlation is a power law with slope close to 0.5, and it was interpreted as X-ray reprocessing from the accretion disk and another extended surface, presumably the companion star (Bernardini et al. 2013; Cackett et al. 2013).

Hynes et al. (2004) showed that (see their Figures 1 and 2) the Hα emission in the BH V404 Cyg in quiescence is positively correlated with the X-ray flux on very short timescales (less than hours, perhaps hundreds of seconds). Moreover, the Hα line is double-peaked, implying that it is produced in the disk. The combination of the two results suggests that the excess optical emission is produced by X-ray irradiation and reprocessing in the disk.

However, at present, a detailed study based on simultaneous OIR and X-ray data of a single object from outburst to quiescence is still missing. Moreover, the population of BH systems as a whole is a factor of $\sim$20 optically brighter than the NS population at a given X-ray luminosity, in both outburst and quiescence (see Figure 2 in Russell et al. 2006). For LMXBs in outburst, Russell et al. (2006, 2007) considered different possibilities, including the size of the accretion disk; however, the differences that arise when comparing BH and NS systems could not be fully explained.

Only simultaneous multifrequency campaigns can help in disentangling the competing emission mechanisms. Here we present and compare for the first time the optical–X-ray correlation of an NS system and a BH system over 6 orders of magnitude in X-ray luminosity, from outburst to quiescence. We selected two transient systems, the BH V404 Cyg (also known as GS 2023+338) and the NS Cen X-4 (also known as V822 Cen). They are the only two transients with simultaneous X-ray and optical data in both outburst and quiescence. For a summary of the main binary system parameters see Table 1.

On 2015 June 15 V404 Cyg entered a new activity period (Barthelmy et al. 2015a, 2015b). The new outburst started between 2015 June 2 and 8, when a faint optical precursor was detected (Bernardini et al. 2015), and it was probably generated by a viscous-thermal instability triggered close to the inner edge of the truncated accretion disk (Bernardini et al. 2016). Near the outburst peak, optical variability was detected on a timescale of tens of minutes (Martí et al. 2016). Subsecond timescale flares were also detected and presumably produced by an optically thin synchrotron jet (Gandhi et al. 2016). The data of the new outburst, which are not analyzed here, can be compared with the results of this work.

2. OBSERVATIONS

We searched the literature for quasi-simultaneous (within a day; $\Delta t \leqslant 1$ day) X-ray and optical observations, which were carried out using the same optical filter in outburst and quiescence. For the X-ray data, we selected the 3–9 keV energy range to match previous studies (see, e.g., Corbel et al. 2008). To convert from count rates and fluxes to luminosities, we used the values of N_H, A_V, and distance (d) reported in Table 1. Moreover, for the outburst X-ray data of both Cen X-4 and V404 Cyg in the hard state, we assume a typical power-law spectral shape, with spectral index $\Gamma = 1.6 \pm 0.1$, as normally used for hard-state sources (e.g., Russell et al. 2006).

For Cen X-4 we used the 1979 outburst data as reported in Russell et al. (2006), where $\Delta t \simeq 0.5$ days. Those are V-band optical monochromatic luminosities, together with 2–10 keV luminosities that we converted to 3–9 keV luminosities using WEBPIMMS.[5] We subtracted the companion star contribution by assuming for it $m_V = 18.4 \pm 0.1$ (dereddened absolute magnitude; Chevalier et al. 1989), which translates to

Table 1
Main Binary Characteristics

Source	Type	Outburst Year	Distance (kpc)	$P_{\rm orb}$ [a] (days)	Incl. (deg)	Companion	M_c [b] ($M_\odot$)	M_p [c] ($M_\odot$)	$N_{\rm H}$ 10^{21} cm^{-2}	A_V
Cen X-4	NS[d]	69, 71, 79 (1)–(3)	1.2 (2), (4), (5)	0.6290522(4) (6)	32^{+8}_{-2} (7)	K3-7V (4), (8)	0.23 ± 0.10 (6)	1.4^e (6), (7)	0.80 ± 0.08 (9)	0.31 ± 0.16 (10)
V404 Cyg	BH	38, 56, 89, 15[f] (11)–(13)	2.39 ± 0.14 (14)	6.4714(1) (15)	67^{+3}_{-1} (16)	K0($\pm$1) III–V (17)–(19)	$0.7^{+0.3}_{-0.2}$ (20)	$9^{+0.2}_{-0.6}$ (21)	12 ± 4^g (22), (23)	4.0 ± 0.4 (18), (19)

Notes. The corresponding references are show in parentheses below each value.
[a] The spin period of Cen X-4 is currently unknown.
[b] Companion mass.
[c] Primary mass.
[d] The detection of an X-ray type I burst during the decay of the 1979 outburst unambiguously showed that this binary hosts an NS (Matsuoka et al. 1980).
[e] This value is in between that measured by Casares et al. (2007), $1.14 \pm 0.45\,M_\odot$, and that measured by Shahbaz et al. (2014), $1.94^{+0.37}_{-0.85}\,M_\odot$.
[f] During 2015 June, the source entered a new outburst state (Barthelmy et al. 2015a), shortly after followed by a second activity period on 2015 December (Barthelmy et al. 2015b).
[g] The uncertainty corresponds to the standard deviation of the values of $N_{\rm H}$ of observations 3–7 reported in Zycki et al. (1999a), together with that of Rana et al. (2015).

References: (1) Conner et al. 1969; (2) Kuulkers et al. 2009; (3) Kaluzienski et al. 1980; (4) Chevalier et al. 1989; (5) González Hernández et al. 2005; (6) Casares et al. 2007; (7) Shahbaz et al. 2014; (8) D'Avanzo et al. 2005; (9) Bernardini et al. 2013; (10) Russell et al. 2006; (11) Makino 1989; (12) Richter 1989; (13) Zycki et al. 1999b; (14) Miller-Jones et al. 2009; (15) Casares & Charles 1994; (16) Khargharia et al. 2010; (17) Wagner et al. 1992; (18) Casares et al. 1993; (19) Hynes et al. 2009; (20) Shahbaz et al. 1994; (21) Khargharia et al. 2010; (22) Zycki et al. 1999a; (23) Rana et al. 2015.

$L_V = 1.55 \pm 0.14 \times 10^{32}$ erg s^{-1}. Quiescent Cen X-4 data are from Bernardini et al. (2013), who used strictly simultaneous optical–UV and X-ray *Swift* data collected between 2012 May and August. We converted the *V*-band count rate to monochromatic luminosity. We first dereddened the optical data and then, as for the outburst data, subtracted the companion star contribution. We converted the quiescent 0.3–10 keV count rate to 3–9 keV luminosity using the average spectrum presented in Bernardini et al. (2013) and the best-fitting spectral model presented in Chakrabarty et al. (2014), which consists of an NS atmosphere component plus a cutoff power law with $\Gamma = 1.02 \pm 0.10$ and $E_{\rm cutoff} = 10.4 \pm 1.4$ keV. We found that 1 counts s^{-1} (0.3–10 keV) corresponds to $L_{3-9\,\rm keV} = 1.28 \pm 0.04 \times 10^{33}$ erg s^{-1}.

For V404 Cyg in outburst (1989), we used the *R*-band luminosity from Russell et al. (2006) adopting the updated source distance and reddening. We also subtracted the companion star contribution ($L_R = 2.53 \pm 0.44 \times 10^{34}$ erg s^{-1}) estimated from the fit to the SED (see Figure 2 and Section 3.2). X-ray data are instead from Corbel et al. (2008); we converted their 3–9 keV fluxes to luminosities. The source showed high-amplitude variability in the first phase of the outburst, with a short transition to a thermal state (see Corbel et al. 2008 and references therein). Consequently, in order to use only data from the hard state where both γ and $N_{\rm H}$ are constant within uncertainty (see observations 3–7 in Table 2 of Zycki et al. 1999a), we limited our analysis to the pointings performed after MJD = 47,685. The *R*-band and X-ray data were quasi-simultaneous. However, by fitting the *R*-band flux decay with an exponential function, which provides a very good description of the decay (as expected in the DIM; Lasota 2001), we were able to estimate the *R*-band luminosity at the exact time of each of the X-ray pointings. Quiescent V404 Cyg data are from Hynes et al. (2004), who used simultaneous optical and X-ray *Chandra* (0.3–7 keV) data collected on 2003 July 28/29. Optical data are taken in two close bands (6300–6500 Å plus 6620–6820 Å) that lie within the *R*-band filter. We converted flux densities to luminosities using the *R*-band central wavelength (6580 Å). We dereddened
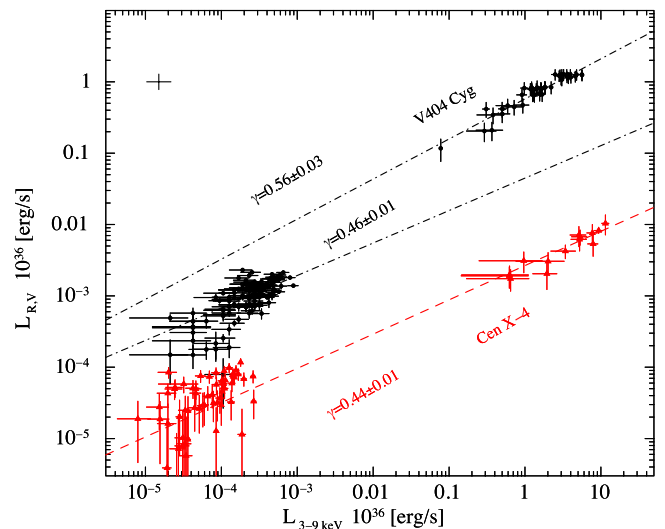

Figure 1. Optical–X-ray (3–9 keV) correlation. Black circles represent V404 Cyg data (*R* band). Red triangles represent Cen X-4 data (*V* band). The black dot-dashed lines are a power-law fit to the V404 Cyg outburst and quiescent data, separately. The red dashed line is a power-law fit over the whole Cen X-4 data set, from outburst to quiescence. The value of the power-law index γ is also reported. In the upper left corner we also show the average systematic uncertainty level, about a factor of 1.44 and 1.28 in optical and X-ray luminosity, respectively (black cross).

using $A_R = A_V \times y = 4 \times 0.751$, where *y* is from Cardelli et al. (1989). In analogy with Hynes et al. (2009) and Zurita et al. (2004), we subtracted the contribution from the companion star by using the lower envelope of the variability to define an upper limit on it. We converted the quiescent X-ray count rate to 3–9 keV luminosity using $\Gamma = 1.85$ (Rana et al. 2015).

In Figure 1 we plot optical ($L_{\rm opt}$) versus X-ray ($L_{3-9\,\rm keV}$) luminosity in units of 10^{36} erg s^{-1} for all data in the present study. Uncertainties are, hereafter, at the 1σ confidence level. In addition, radio to optical/UV data were collected to construct SEDs of Cen X-4 and V404 Cyg (see Figure 2 for data
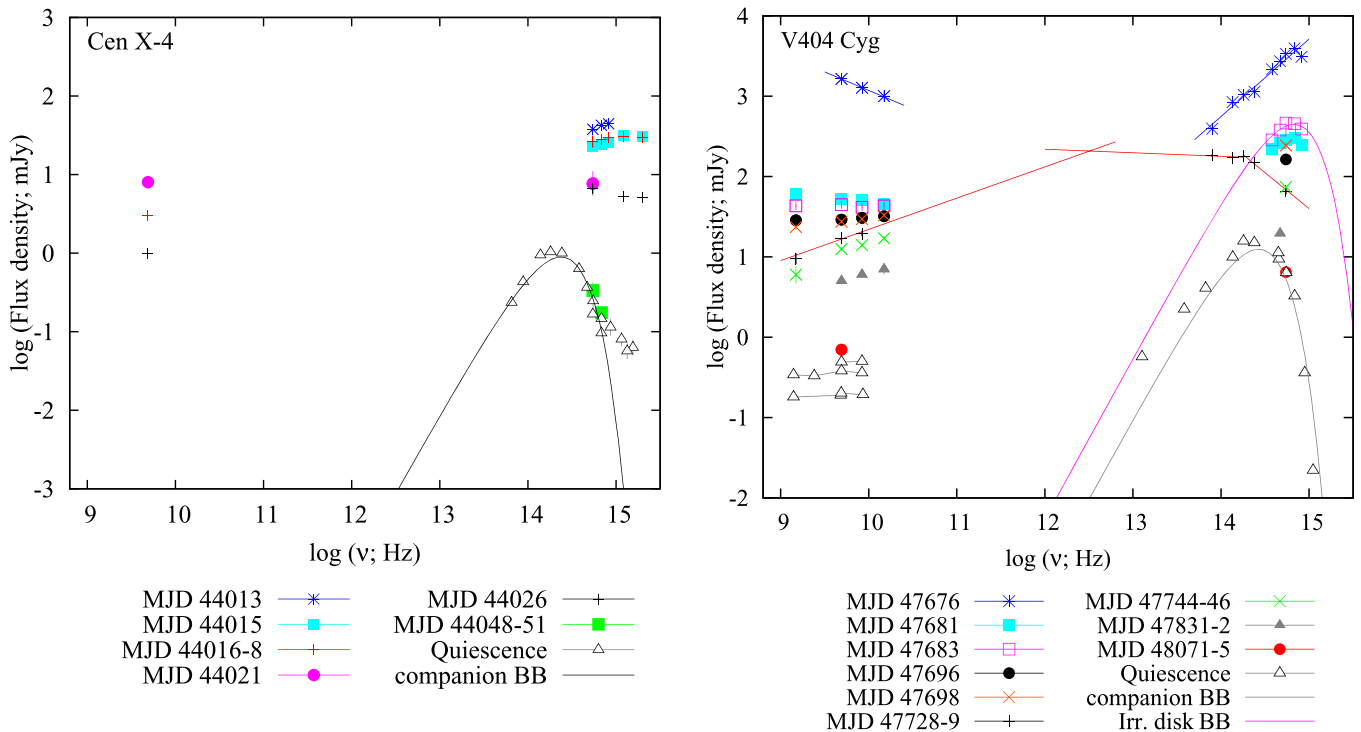
Figure 2. Left panel: broadband, radio to optical (dereddened) spectra of Cen X-4 during its 1979 outburst and quiescence. The black line is a blackbody with a temperature of 4050 K representing the companion star. Data are from Blair et al. (1984), Bernardini et al. (2013), Canizares et al. (1980), Hjellming (1979), Kaluzienski et al. (1980), Shahbaz et al. (1993), van Paradijs & McClintock (1994), and Wang & Wang (2014). Right panel: broadband, radio to optical (dereddened) spectra of V404 Cyg during its 1989 outburst and quiescence. The first spectra were obtained near the peak of the outburst, and in general, time progresses from top to bottom. The red lines show the fit to the jet spectrum obtained on MJD 47,728–29 (Russell et al. 2013), and the gray and purple curves show single-temperature blackbody approximations to the data in quiescence and on MJD 47,683, respectively. The radio data are taken from Han & Hjellming (1992), Gallo et al. (2005), and Hynes et al. (2009); the gray lines joining radio data points are taken on the same dates. The infrared, optical, and UV data are from Gehrz et al. (1989a, 1989b), Casares et al. (1991, 1993), Leibowitz et al. (1991), Udalski & Kaluzny (1991), Wagner et al. (1991), Han & Hjellming (1992), and Hynes et al. (2009).

references). The IR–optical–UV data were dereddened using the law of Cardelli et al. (1989) as above. Data used for the SEDs were taken within a day, unless stated otherwise, by a range of MJD values in Figure 1 and Table 3; quiescence data were taken on several dates.

3. RESULTS

3.1. Optical–X-Ray Correlations

In order to assess whether an optical–X-ray luminosity correlation is present, in both outburst and quiescence, and find out whether the same correlation (e.g., a single power law) extends across the two states, we used the following procedure. We first fitted, separately, the quiescent and outburst data with a power-law model, $y = ax^{\gamma}$, and we compared the two derived slopes (γ) and normalizations (a). Then, if these were found to be consistent with each other, we fitted together the whole data set, covering about six orders of magnitude in X-ray luminosity. To measure the statistical significance of the correlation, we used a Spearman's rank correlation test. We report the Spearman's correlation coefficient ρ, the null hypothesis probability P, γ, and a in Table 2.

For Cen X-4 in both outburst and quiescence, the Spearman's rank test shows that the V-band and X-ray data are positively correlated. Moreover, the two power laws are consistent within 1σ uncertainty in Γ and within 2σ in a. Consequently, we performed a single fit over the whole luminosity range. For V404 Cyg, in both cases, Spearman's

Table 2
Correlation Fit Results

State	γ	a	ρ	P (σ)[a]
Cen X-4				
O	0.58 ± 0.08	0.0022 ± 0.0003	0.92	4.1×10^{-6} (4.5)
Q	0.50 ± 0.06	$0.005^{0.004}_{0.002}$	0.55	4.7×10^{-6} (4.4)
O–Q	0.44 ± 0.01	0.0028 ± 0.0002	0.76	2.2×10^{-15} (>8)
V404 Cyg				
O	0.56 ± 0.03	0.58 ± 0.02	0.91	3.6×10^{-18} (>8)
Q	0.46 ± 0.01	0.045 ± 0.003	0.68	3.8×10^{-19} (>8)

Note. O is outburst (hard state), Q is quiescence, and O–Q is the two data sets combined. The fit is made with a power law of the form $y = ax^{\gamma}$, while ρ is Spearman's correlation coefficient.
[a] In parentheses we report the confidence level in σ.

rank test shows that the R-band and X-ray data are positively correlated. However, while the two power-law slopes are barely consistent within 3σ, the two normalizations are inconsistent, the one from the outburst being much higher. If we extrapolate the outburst best-fitting power law downward to the bottom range of the explored X-ray luminosity (at $L_X = 1.5 \times 10^{31}$ erg s^{-1}), we find that the measured quiescent optical luminosities are a factor of $\sim$4.0 fainter than expected. If we do the opposite and extrapolate upward the best-fitting quiescent power law to $L_X = 5.7 \times 10^{36}$ erg s^{-1}, we find a

factor of ∼15 difference. In Figure 1 we also show the best-fitting power-law models.

We conclude that a single, positive correlation, with a slope $\gamma = 0.44 \pm 0.01$, extending from outburst to quiescence represents well the Cen X-4 data. For V404 Cyg, instead, the slope of the correlation slightly decreases from outburst ($\gamma = 0.56$) to quiescence ($\gamma = 0.46$). However, the optical quiescent data are a factor of 4–15 fainter than expected, based on the outburst correlation alone. Moreover, when directly comparing V404 Cyg and Cen X-4, the optical luminosity of the BH correlation is a factor of about 160–280 higher than that of the NS in outburst (the values of 160 and 280 are measured at $L_X = 1 \times 10^{35}$ erg s^{-1} and $L_X = 1 \times 10^{37}$, respectively). This factor is about 10 times smaller in quiescence.

3.1.1. Systematic

In the top left corner of Figure 1 we show the average (between Cen X-4 and V404 Cyg outburst and quiescent data) systematic uncertainty, a factor of 1.44 and 1.28 in optical and X-ray luminosity, respectively. The X-ray systematic is the combination in quadrature of the uncertainties of the distance, the absorption, and the spectral shape (the uncertainty on the power-law photon index for V404 Cyg and on the conversion factor from 0.3–10 keV counts s^{-1} to $L_{3-9\,keV}$ for Cen X-4). In the case of the optical data it includes the uncertainty in the distance, the extinction, the characterization of the companion star lower envelope (∼10% for V404 Cyg), and a factor of 10% systematic error in the measure of the quiescent flux (for V404 Cyg). The total uncertainty in X-ray and optical luminosities is the combination in quadrature of the uncertainty of the X-ray and optical fluxes (plotted on each point) and the systematics. The effect of the systematics is not included in the correlation analysis for each source, nor in the following sections, e.g., when fitting the corrected correlations.

3.2. SEDs

The optical emission processes in outburst and quiescence can also be constrained by identifying components in the broadband spectrum. In Figure 2 we present the radio to optical/UV broadband spectra of V404 Cyg and Cen X-4 during outburst and quiescence taken from the literature. Displayed spectra are those in which multiple bands were observed on or around the same dates (the date ranges are given in the figure key).

3.2.1. V404 Cyg

The continuum optical emission of V404 Cyg close to the outburst peak (MJD 47,676) was dominated by a blue component ($\alpha_{opt} > 0$), which is plausibly due to X-ray heating of the accretion disk, whereas during the decay (e.g., MJD 47,728–29) the continuum was redder ($\alpha_{opt} < 0$) and consistent with a jet synchrotron spectrum (see also Wagner et al. 1991; Russell et al. 2013). Both components are visible in the spectrum at different stages of the outburst decay. In the soft state (MJD 47,676), the radio emission was bright and optically thin ($\alpha_{rad} < 0$; probably originating from discrete ejections), and its (power-law) extrapolation cannot make a significant contribution to the optical emission. As the source faded and returned to the hard state, the radio spectrum flattened (MJD 47,681–47,683) and then became inverted (MJD $\geqslant$ 47,696), a behavior typical of the steady, compact jets

commonly seen in the hard state (Han & Hjellming 1992; Corbel et al. 2008). The maximum possible jet contribution to the optical emission, as estimated by extrapolating the radio power law, increased with time as the source evolved from the soft to the hard state. The flux of the irradiated disk component also decreased. In Table 3 the estimated star, disk, and jet contributions are given for each date when these parameters can be constrained by the data. We report the value in the V band, which is where most data are available (the derived percentages are consistent in the R band).

In the following we describe in detail the way in which we estimate the companion star, disk, and jet contribution in V404 Cyg for each date. The quiescent companion star is modeled as a blackbody at a temperature of 4570 K with a normalization that assumes that 86.5% of the quiescent R-band flux is stellar light (see Hynes et al. 2009 and references therein). The contribution of this blackbody to the V-band flux on each date is first estimated. The maximum jet contribution is the flux density of the extrapolated radio power law as a fraction of the observed flux density, with the quiescent companion contribution subtracted. The disk contribution is constrained from the remaining part of the observed flux density that cannot be accounted for by the star or jet. Before the transition to the hard state (MJD < 47,683), the jet made only a minimal contribution to the optical flux, <10%. The optical spectrum was also blue and can be very crudely fitted by a single-temperature blackbody (one example is shown; on MJD 47,683 the spectrum can be described by a ∼11,500 K blackbody), which most likely represents irradiation on the disk surface (e.g., Hynes et al. 2009).

From MJD 47,698 onward, the jet could account for more than 50% of the V-band flux density, and on the only date on which more than one optical/IR filter was acquired (MJD 47,728–29), it is red and inconsistent with a blackbody. Instead, the fluxes on this date can be described by a jet spectrum with a break at infrared frequencies (Russell et al. 2013). Since the V-band flux density ($\sim 6 \times 10^{14}$ Hz) was considerably lower than the infrared ($\sim 10^{14}$ Hz) flux densities, and the infrared–optical spectral index was $\alpha_{thin} = -0.89 \pm 0.11$, the disk contribution was plausibly low at this time. This spectral index represents the slope of the optically thin synchrotron emission near the jet base if there is no disk contribution. As a further check, we explored a wide range of possible disk contributions (0%–40%) and see how the jet spectral index would change accordingly. Then, we rejected those jet spectral index values that, also based on the comparison with other BHXBs, are unlikely (see below). In Figure 3 we show the spectral index α_{thin} of the jet spectrum as a function of the V-band contribution of the irradiated disk (the low-level contribution of the star has been subtracted from each waveband before fitting). If the disk contributed more than ∼10% of the V-band flux, the jet spectral index would be steeper, $\alpha_{thin} < -1.0$; a disk contribution of 40% would translate to $\alpha_{thin} = -1.5 \pm 0.2$. Such a steep index is unusual, but not unheard of. A recent compilation of measurements of α_{thin} from BHXBs shows that the spectral index is typically -0.7 to -0.8, but can be as steep as -1.4 (Russell et al. 2013). However, all the sources with $\alpha_{thin} \leqslant -1.0$ accrete at low luminosity ($L_X \leqslant 5 \times 10^{-3} L_{Edd}$; see also Shahbaz et al. 2013), and in one source α_{thin} was seen to increase with luminosity, and the steeper indices could be explained by a contribution of thermal particles in the jet at low accretion rates (Russell

Table 3
Evolution of the Irradiated Disk, and Jet Contributions, before (I) and after (II) the Subtraction of the Contribution of the Companion Star, to the Optical (*V*-band) Emission of V404 Cyg as Estimated from the Broadband Spectra

MJD	Spectral State	*V*-band Flux Density (mJy)	Irradiated Disk (I) (%)	Jet (I) (%)	Star (%)	Irradiated Disk (II) (%)	Jet (II) (%)
47,676	Soft	3361	$\geqslant$99.6	<0.2	0.2	$\geqslant$99.8	<0.2
47,681	Soft to Hard	285	$\geqslant$92.8	<5.4	1.8	$\geqslant$94.5	<5.5
47,683	Soft to Hard	464	$\geqslant$90.3	<8.6	1.1	$\geqslant$91.3	<8.7
47,690	Hard	324	$\geqslant$66.2	<32.2	1.6	$\geqslant$67.3	<32.7
47,696	Hard	163	$\geqslant$65.0	<31.8	3.2	$\geqslant$67.1	<32.9
47,698	Hard	243	$\geqslant$37.5	<60.3	2.2	$\geqslant$38.3	<61.7
47,711–13	Hard	15.5	…	<66.2	33.8	…	<100
47,728–9	Hard	65.8 ± 6.1	$\leqslant$14.0	78.0–92.0[a]	8.0	0–15	85–100
47,744–6	Hard	73.9 ± 1.7	…	$\leqslant$92.9	7.1	…	$\leqslant$100
47,831–2	Hard	19.6 ± 0.7[b]	…	$\leqslant$58.7	41.3	…	$\leqslant$100
48,052	Hard	9.5 ± 0.4	…	$\leqslant$44.8	55.2	…	$\leqslant$100
48,071–5	Hard	~6.5	$\leqslant$19	$\leqslant$19	~81	$\leqslant$100	$\leqslant$100
Various	Quiescence	6.35 ± 0.12	5.5–17.4	<11.9[c]	82.6	31.6–100	<68.4

Notes. All flux densities are dereddened. The soft-to-hard state transition occurred around MJD 47,680–85.
[a] Assumes that the maximum disk contribution is 13.4% of the observed *V*-band flux, which is implied by the inferred slope of the optically thin synchrotron jet emission (see the text).
[b] *R*-band flux densities (no *V*-band data available).
[c] The jet contribution is <11.9%, <5.9%, and <3.0% using the brightest, central, and faintest radio SEDs, respectively.
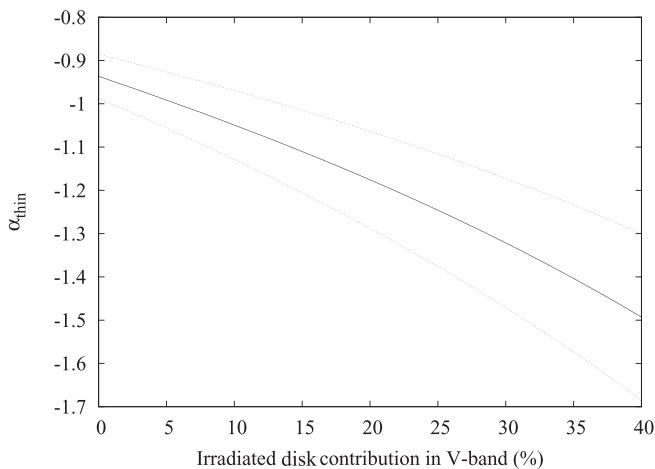
Figure 3. Spectral index $\alpha_{\rm thin}$ of the optically thin synchrotron emission from the jet at optical–IR frequencies on MJD 47,728–29 as a function of the contribution of the irradiated disk in the *V* band. If the disk contribution exceeds ~14% of the flux, $\alpha_{\rm thin} < -1.0$, which is steeper than expected at this luminosity.

et al. 2010; Shahbaz et al. 2013). If this were the case, then we would not expect the spectral index of the jet in V404 Cyg to be steep at the time of this broadband spectrum because its luminosity was high, with $L_{\rm X} = 2 \times 10^{-2} L_{\rm Edd}$. If $\alpha_{\rm thin} \geqslant -1.0$, then the disk contributed less than ~14% of the *V*-band flux (Figure 2), with the jet contributing 78%–92%. We suspect that there must be some disk contribution, because we would not expect the disk to fade so rapidly compared to the jet, so we estimate the disk contribution to be ~10% ± 4% on MJD 47,728–29.

In quiescence, the radio spectrum appears to be approximately flat on three dates (see also Gallo et al. 2005; Hynes et al. 2009), but the normalization changes, ranging from 0.19 to 0.5 mJy, demonstrating jet variability in quiescence (see also Hynes et al. 2009). Even higher radio flux densities up to

1.5 mJy have been reported (Hjellming et al. 2000) and imply a radio flux range of a factor of ~8 (but we do not include it in the right panel of Figure 2, because no radio frequency was reported). There is an excess of mid-IR emission (in the range 10^{13}–10^{14} Hz) above the star blackbody, which could originate in the jet if the flat radio spectrum extends to mid-IR frequencies (see Figure 2, right panel; see also Gallo et al. 2007; Hynes et al. 2009). By extrapolating the three radio spectra to higher frequencies, we are able to estimate the maximum contribution of the jet to the quiescent optical emission, which must be at maximum 3%–12% in *V* band depending on the choice of radio spectrum (in Table 3, the values for the middle of the three radio spectra are shown). The disk contributes up to 17%, with the star producing the majority of the quiescent flux (see also Pavlenko et al. 1996; Shahbaz et al. 2003; Hynes et al. 2004, 2009; Zurita et al. 2004; Gallo et al. 2007; Xie et al. 2014).

3.2.2. Cen X-4

The SEDs of Cen X-4 are shown in the left panel of Figure 2. During outburst, optical and UV fluxes were measured, but only three radio detections were reported, and no infrared data were taken. Near the outburst peak (MJD 44,013–18), the optical emission was dominated by a blue component ($\alpha > 0$), similar to V404 Cyg. This component appears to peak (in flux density) in the near-UV, which may be the peak of the irradiated disk component (see Blair et al. 1984), also seen in some BHXBs (e.g., Hynes 2005). As the source faded during the outburst decline, the flux varied by a factor of ~8 in 5 days at radio frequencies (MJD 44,021–26), while the optical flux remained constant (within errors) during the same dates. This suggests that the jet emission is unlikely to dominate the optical emission; otherwise, one might expect a variable optical flux of similar amplitude. The optical spectral index became slightly redder as the source faded (MJD 44,026), possibly due to the peak of the irradiation blackbody shifting to lower frequencies (the spectral index is bluer than expected for optically thin synchrotron emission from the jet).

In quiescence, both the companion star and disk contribute to the IR–optical–UV SED (see also Bernardini et al. 2013; Baglio et al. 2014; Wang & Wang 2014). The IR SED can be well fit by a single-temperature blackbody from the companion star, with an effective temperature of 4050 K (Baglio et al. 2014; also shown in Figure 2 of this paper). The optical–UV flux excess above the companion correlates with the X-ray flux (Bernardini et al. 2013; Cackett et al. 2013), which can be explained by reprocessing. Stringent upper limits on the flux and polarization of the jet at optical–IR frequencies have also been reported (less than 10%; Baglio et al. 2014).

We conclude that for Cen X-4 the jets have made a negligible contribution to the optical emission in outburst and quiescence.

4. DISCUSSION

During outburst, we found that the optical luminosity of the BH system V404 Cyg is a factor of about 160–280 higher than that of the NS system Cen X-4, for a given X-ray luminosity. During quiescence, this factor is 10 times smaller. Moreover, we found that the normalization of the correlation of V404 Cyg changes between outburst and quiescence (see Figure 1).

We now explore what physical mechanisms can produce a higher optical flux in the BH system and the change in the slope and normalization of its L_X–L_{opt} correlation. In particular, our goal is to test whether the L_X–L_{opt} correlations of V404 Cyg and Cen X-4 overlap, once the main known differences between the two systems are taken into account. To this aim, we discuss and apply one by one the relevant corrections to the observed correlation adopting Cen X-4 data as a benchmark.

4.1. Corrections to the Optical–X-Ray Correlation

4.1.1. Bolometric X-Ray Emission

The flux in the 3–9 keV range is just a fraction of the total X-ray flux (F_{bol}), for which we adopt the 0.5–200 keV range. $F_{3-9\,keV} = F_{0.5-200\,keV} \times \xi$, where ξ is the bolometric correction factor. Migliari & Fender (2006) provide the value of ξ for BHXBs and NSXBs in outburst, depending on the source type and spectral state, with the caveat that they derived ξ by referring to the 2–10 keV flux (instead of 3–9 keV). Their values are $\xi = 0.20 \pm 0.02$ for the BH hard state, which includes the contribution of reflection (Nowak et al. 2002),[6] and $\xi = 0.40 \pm 0.04$ for NS Atoll sources in the hard state. While Cen X-4 has not yet been properly classified (see Hasinger & van der Klis 1989; Ritter & Kolb 2003, for the atoll source definition and a catalog of LMXBs with their classification, respectively), the detection of a type I burst (Matsuoka et al. 1980) strongly suggests that Cen X-4 is a member of the Atoll class. Therefore, we assume that Cen X-4 is an Atoll source. In order to estimate the bolometric correction in quiescence, we used, for Cen X-4, the *Swift* X-ray data presented in Bernardini et al. (2013). The *Swift* observations, when summed together, provide the most extensive look at the source quiescence currently available (~110 ks). More recently, thanks to the high-energy sensitivity

of the *NuSTAR* observatory in the hard X-rays, Chakrabarty et al. (2014) identified a spectral cutoff at ~10.4 keV in the spectrum of Cen X-4 in quiescence. We applied their spectral model, consisting of an NS atmosphere plus a cutoff power law (spectral index 1.02), to the total *Swift* X-ray spectrum. We extrapolated the model to the 0.5–200 keV range, compared the derived unabsorbed flux with that measured in the 3–9 keV range, and derived $\xi = 0.16 \pm 0.02$.

For V404 Cyg, we used the *Swift* X-ray data (~140 ks) presented in Bernardini & Cackett (2014) and a model consisting of a power law with spectral index 1.85 with a cutoff at 19 keV. This is what was recently found in quiescence using simultaneous *XMM-Newton* and *NuSTAR* by Rana et al. (2015). We extrapolated the spectral model to the 0.5–200 keV range, compared the unabsorbed flux with that in the 3–9 keV range, and found $\xi = 0.28 \pm 0.03$.

4.1.2. X-Ray Reprocessing

We found that for Cen X-4 a single power-law correlation with a slope γ close to 0.5 extends over six orders of magnitude in X-ray luminosity, suggesting that the same physical mechanism(s) operate(s) during outburst and quiescence. Bernardini et al. (2013) showed that during quiescence the X-ray and optical–UV fluxes are strongly correlated on a timescale probably[7] shorter than the viscous timescale (see also Cackett et al. 2013). This suggests that the optical (and UV)–X-ray correlation in quiescence is due to reprocessing and not to thermal instabilities propagating through the disk. The slope of the correlation can also provide constraints on the underlying emission mechanisms. Van Paradijs & McClintock (1994) showed that in the case of disk reprocessing the optical luminosity scales with the X-ray luminosity following the relation $L_V \propto L_X^\gamma R$, where R is the accretion disk outer radius and $\gamma = 0.5$ (see also Shahbaz et al. 2015, for the way γ changes in different frequency bands). For Cen X-4, γ is very close to 0.5, suggesting that X-ray reprocessing in the disk may be responsible for the optical luminosity. Consequently, we start assuming that X-ray reprocessing from the disk has a relevant role in the correlation and see whether this effect can account for the difference in optical luminosity between Cen X-4 and V404 Cyg. We stress that within uncertainty also the slope of the correlation of the BH V404 Cyg, in both outburst and quiescence, is consistent with X-ray reprocessing. From van Paradijs & McClintock (1994), by using Kepler's third law, we have $L_{opt} \propto L_X^{1/2}(M_p + M_c)^{1/3}P^{2/3}$, where M_p and M_c are the primary (compact object) and companion mass, respectively. We find L_{opt}(V404 Cyg)/L_{opt}(Cen X-4) ~ 8–9 (the range mainly depends on the NS mass estimate, which is 1.14 and 1.94 according to Casares et al. [2007] and Shahbaz et al. [2014], respectively). Once the V404 Cyg data are corrected for this effect (we used 8.5, which corresponds to an NS of 1.4 $M_\odot$) and the X-ray bolometric emission is considered, the two sets of quiescent data are much closer to each other, but there is still a factor of ~20 difference in optical luminosity during outburst (see Figure 4, left panel). We conclude that X-ray reprocessing alone cannot account for the difference in optical luminosity in outburst and that some further mechanism must make the BH system optically brighter.

---

[6] To estimate the BH hard-state conversion factor, Migliari & Fender (2006) used data from GX 339-4 presented in Nowak et al. (2002), where reflection is clearly present. The reflection amplitude is correlated with the X-ray flux for GX 339-4 as it is for V404 Cyg (see Zycki et al. 1999a). Nowak et al. (2002) concluded that the correlation between X-ray flux and reflection is a general property of BH transients in the hard state.

---

[7] The real structure of the quiescent disk is unknown, and consequently the viscous timescale is hard to constrain.
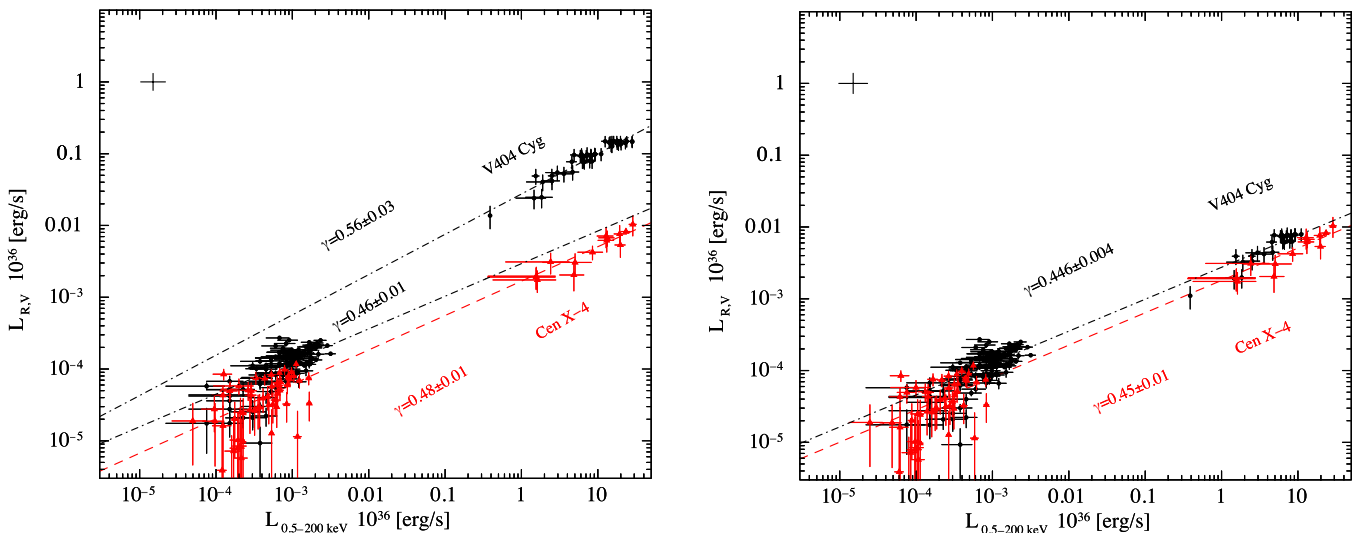
Figure 4. Optical–X-ray (0.5–200 keV) correlation. In both panels we used Cen X-4 as a benchmark. Left panel: same as Figure 1, but including the correction for orbital parameters (star masses and orbital period) and for the bolometric X-ray luminosity, which both affect the amount of optical emission we expect from reprocessing on the disk. Note that we have normalized the BH optical luminosity by a factor of 1/8.5 to account for the different disk sizes (see the text for more details). The average systematic uncertainty level is a factor of 1.45 and 1.31 in optical and X-ray luminosity, respectively (black cross). Right panel: same as the left panel, but first subtracting the jet contribution for V404 Cyg in outburst (92% of the *R*-band luminosity once the companion star has been subtracted) and the contribution from the NS surface in quiescence for Cen X-4 (50% of the 0.5–200 keV luminosity) and then dividing by 8.5. For V404 Cyg in outburst hard state, we are only plotting the observations where the jet is dominating (MJD ⩾ 47,711) the emission at optical frequencies. The average systematic uncertainty level is a factor of 1.54 and 1.38 in optical and X-ray luminosity, respectively (black cross).

4.1.3. Synchrotron Jet Emission

In the following we try to identify which other mechanism can make V404 Cyg optically brighter with respect to Cen X-4. The SED of V404 Cyg in the hard state clearly reveals the presence of an optically thick synchrotron jet. Moreover, jet emission is plausibly detected at optical frequencies also in the flares of the 2015 outburst (see, e.g., Hynes et al. 2015). We showed that optical emission in the hard state is very likely jet dominated starting from MJD 47,711 (see Table 3). From the SED where the jet break is found (MJD 47,728–29), we estimate that the companion-subtracted jet contribution in the optical *V* band is 85%–100%. We assume that this range of values also applies to all the following hard-state observations in the time range 47,711–48,075 MJD. The companion-subtracted jet contribution is instead much lower during quiescence, and the disk is probably dominating at optical frequencies (31.6%–100%).

Cen X-4 was detected at radio frequencies ($\sim 4.9 \times 10^9$ Hz) during outburst. The SED in the optical is fairly blue, likely due to a dominant disk contribution. There is no radio detection for Cen X-4 in quiescence, nor is there any evidence for an optical–IR excess from the jet in Cen X-4 (see also Baglio et al. 2014; Wang & Wang 2014). Moreover, NS LMXBs presumably do not attain a jet-dominated state during quiescence (Gallo et al. 2012). The optical SEDs of Cen X-4 in outburst have a shape consistent with disk emission, a similar result to other NS systems in outburst. Any synchrotron emission would contribute significantly only at frequencies lower than the optical/IR bands in the case of Cen X-4 (Maitra & Bailyn 2008; Lewis et al. 2010; Migliari et al. 2010). We conclude that the jet contribution to the optical emission in outburst and quiescence for Cen X-4 is negligible. Summarizing, the comparison of the SED of V404 Cyg and Cen X-4 suggests that the jet is mainly responsible for shaping the difference between the two sources in outburst.

In the following we test whether the slope of the correlation confirms these results. When comparing X-ray and optical (*R*-band) emission for the BH V404 Cyg in outburst, before applying any correction (see the uncorrected correlation in Figure 1) we get $\gamma = 0.56$. Corbel et al. (2008) found for V404 Cyg a power-law correlation with an index $\gamma = 0.51$, extending from outburst to quiescence, based on the comparison of simultaneous radio and X-ray data. They conclude that the correlation is produced by the emission from a compact jet. The value they found is fully consistent with what we found in outburst. Han & Hjellming (1992) show that the spectral index of the self-absorbed, optically thick, synchrotron jet (α_{thick}) in the radio band during the hard-state decay of the 1989 outburst of V404 Cyg was between ~ 0.2 and ~ 0.6 (see also Russell et al. 2013). We can use the 0.2–0.6 range to derive the expected theoretical relation between $L_{\nu,\text{radio}}$ (radio monochromatic luminosity at a given frequency) and L_X for the case in which the jet is dominating the emission at these frequencies. Following the analytic model presented by Heinz & Sunyaev (2003), assuming that the jet in the hard state is radiatively inefficient with $L_X \propto \dot{m}^2$, that the radiative efficiency is not changing with luminosity, and that the jet power is a constant function of the power released by accretion, we have $L_{\nu,\text{jet}} \propto \dot{m}^{\left(17/12 - \frac{2}{3}\alpha_{\text{thick}}\right)}$ (see Equation (7) in Russell et al. 2013). Rearranging for L_X, we have $L_{\nu,\text{jet}} \propto L_X^{0.51-0.64}$. Since the jet spectrum extends to optical/IR frequencies, and since there is no strong dependency of the jet break frequency on luminosity (Russell et al. 2013), we expect this relation to hold also in the optical band ($L_{\nu,\text{jet}} \propto L_{\text{opt}}$). Summarizing, from both an observational (see Corbel et al. 2008) and a theoretical (Heinz & Sunyaev 2003) point of view, in the jet case we expect a power-law relation between optical and X-ray luminosity with an index γ very close to 0.5–0.6. This is indeed what we measure in outburst ($\gamma = 0.56$), while, during quiescence, we measure a slightly lower value ($\gamma = 0.46$).

Table 4
Summary of All Corrections Applied to the Raw Data in Figure 1 (Uncorrected Correlation) to Get Figure 4, Right Panel (Corrected Correlation)

Source	ξ [a]	Jet[b]	Disk Size[b]	NS Surface[a]
Quiescence				
Cen X-4	×6.3	...	...	÷2
V404 Cyg	×3.6	...	÷8.5	...
Outburst				
Source	ξ	Jet	Disk Size	NS Surface
Cen X-4	×2.5	...	...	...
V404 Cyg	×5	×0.08	÷8.5	...

Notes. ξ is the X-ray bolometric correction.
[a] Correction applied to the X-ray data.
[b] Correction applied to the optical data.

Starting from the uncorrected correlation, in order to remove the jet contribution in the outburst hard state, we consider that the jet produces 92% of the optical emission (the mean of the estimated range when the companion contribution is subtracted). Once the jet contribution is removed and the X-ray bolometric correction is applied, the outburst data of V404 Cyg appear to be closer to those from Cen X-4, but a difference of about one order of magnitude still remains. We notice that this corresponds to the difference expected if X-ray reprocessing in the disk takes place.

Let us now take a closer look at the two systems in quiescence. The X-ray spectrum of the BH V404 Cyg is well fitted by a simple power-law model, while that of the NS Cen X-4 is more complex. In addition to the power-law component, there is also a thermal contribution arising from the NS surface. We estimate that the two components provide 50% each of the 0.5–200 keV quiescent X-ray luminosity, in agreement with the results of Bernardini et al. (2013). Since BHs do not have a radiating solid surface, in order to properly compare V404 Cyg and Cen X-4 in quiescence, we need to also remove the X-ray luminosity that arises from the NS surface.

We can look at the right panel of Figure 4 (i.e., corrected correlation) as a comparison of the correlation of V404 Cyg and Cen X-4 once the jet emission and the emission from the NS surface have been removed, and assuming that the two systems have the same disk size. We also report in Table 4 the intensity of all corrections we applied to generate this plot, starting from the raw data presented in Figure 1 (uncorrected correlation). In more detail, for V404 Cyg we first account for the jet contribution in the hard state (subtracting 92% of the optical luminosity), which we have shown is the dominant emission process at this frequency starting from MJD 47,711 (we are now only using observations from this date on). Then, we account for the difference in orbital parameters, namely, the primary and secondary masses and orbital period (dividing the optical luminosity by 8.5), and for the bolometric X-ray correction. For Cen X-4 we also remove the blackbody-like contribution from the NS surface in quiescence (dividing the X-ray quiescent luminosity by 2) and keep only the power-law spectral component. We notice that the outburst non-jet optical data and quiescent data of V404 Cyg now lie on the same correlation with $\gamma = 0.446 \pm 0.004$. We further notice that Cen X-4 and V404 Cyg now display two correlations that perfectly match each other within 1σ uncertainty (Cen X-4 has

$\gamma = 0.45 \pm 0.01$). We notice that both correlations have a slope close to 0.5, which is what is expected from X-ray reprocessing in the disk. It could also be consistent with a viscously heated disk case, where $L_X \propto L_{\mathrm{opt\text{-}UV}}^{0.3-0.6}$ (Shahbaz et al. 2015). However, we emphasize that in quiescence the optical emission of V404 Cyg (Hynes et al. 2004) and the optical–UV emission of Cen X-4 (Bernardini et al. 2013; Cackett et al. 2013) are correlated with that in the X-ray on a short timescale (hundreds of seconds only for V404 Cyg), strongly suggesting that it is produced by X-ray reprocessing and not by an instability propagating in the disk on the viscous timescale, which is probably much longer than that.

We conclude that during the outburst hard state of V404 Cyg, two main mechanisms, jet (dominant) and X-ray reprocessing, are responsible for the L_X–L_{opt} correlation. During quiescence, instead, the jet contribution is minimal, and the X-ray reprocessing dominates. We ascribe to this the change in the normalization (and slope) in the uncorrected correlation (see Figure 1). For Cen X-4, X-ray reprocessing is likely the dominating emission process in both outburst and quiescence. However, to confirm that disk reprocessing is taking place, we also need to carefully compare the energetics (see Section 4.2).

4.1.4. Inclination and Outer Disk Vertical Size

The amount of reprocessed light in the disk that reaches a far observer is proportional to $\cos(i)$, where i is the binary system inclination with respect to the line of sight. Taking the values from Table 1 ($i = 32°$ and $i = 67°$ for Cen X-4 and V404 Cyg, respectively), we expect Cen X-4 to be a factor of ~2 optically brighter with respect to V404 Cyg for a given X-ray input due to this effect only. However, we point out that i is model dependent and varies from paper to paper, e.g., Shahbaz et al. (1994) found $i = 52° \pm 4°$ for V404 Cyg. Moreover, the orbital inclination of Cen X-4 is not well constrained, and within ~2.5σ it is consistent with 52°. We conclude that the V404 Cyg correlation should be up-shifted by a factor of $\leqslant 2$, depending on the exact value of its inclination.

The amount of reprocessed light from a geometrically thin irradiated disk, in the approximation of an X-ray point-like source located in its center in the disk plane, scales with $(H/R)_{\mathrm{ext}}$, where H and R are the vertical size (semithickness) and the radius of the disk calculated at its outer edge, respectively (see, e.g., Section 5.4.4 in Bernardini et al. 2013, for more details). We highlight that the geometry of the central X-ray source is not known; however, even if it is extended (e.g., a Comptonizing corona), it would remain almost point-like when seen by the outer disk. In turn, H/R is proportional to $\dot{M}^{3/20}$ and $R^{2/7}$ (see Equation (5.49) in Frank et al. 2002), where $\dot{M} = L_X/\eta \, c^2$, $\eta \sim 0.1$ is the efficiency, and the outer radius is of the order of 10^{11} and 10^{12} cm for Cen X-4 and V404 Cyg, respectively. We explored how H/R changes with the X-ray luminosity for V404 Cyg and Cen X-4 from outburst to quiescence and found that for a given X-ray luminosity Cen X-4 should be only a factor of 1.1–1.2 optically brighter. Moreover, we also found that in quiescence, for reasonable values of the viscosity parameter (e.g., $0.0001 < \alpha < 1$), the maximum amount of reprocessed luminosity is $\lesssim 2\%$.

We conclude that the effects due to the inclination and to the outer disk vertical size are minimal when comparing V404 Cyg with Cen X-4 in quiescence and outburst (hard state). Consequently, we do not further correct the right panel of

Figure 4 for these effects. We stress that for other sources the inclination can be accounted for (when it is well constrained), but the disk semithickness is model dependent and largely unknown for most sources, including V404 Cyg and Cen X-4 (this is especially true in quiescence, where the structure of the disk is still unclear).

4.1.5. How to Generate Figure 4, Right Panel

Here we summarize, step by step, the method and equations we used to generate the right panel of Figure 4 (corrected correlation), starting from the raw data (uncorrected correlation) and adopting Cen X-4 as a benchmark. This may be useful to update this figure in the future, including, e.g., more data from other LMXBs or new outburst data from V404 Cyg and Cen X-4.

By transforming the observed correlations, we now aim at sketching a "standard" correlation that would hold for disk reprocessing only for LMXBs containing a BH or an NS, with (I) a given bolometric luminosity; (II) emission from the jet removed; (III) a given accretion disk size (which in turn implies a given primary mass, secondary mass, and orbital period); (IV) emission from the NS surface removed; and (V) a given inclination with respect to the line of sight.

(I) The bolometric X-ray luminosity should be calculated using $F_{3-9\,\mathrm{keV}} = F_{0.5-200\,\mathrm{keV}} \times \xi$, where ξ is 0.4 for NS systems in outburst and 0.2 for BH systems in the outburst hard state. In quiescence we used 0.16 and 0.28 for Cen X-4 and V404 Cyg, respectively. ξ should be estimated for each system in quiescence when possible.

(II) The jet emission contribution at optical frequency should be removed (in both outburst and quiescence, if present). For V404 Cyg in the outburst hard state it is 92% of the companion-subtracted optical flux.

(III) The jet-subtracted optical emission should be normalized to that of Cen X-4 using $L_{\mathrm{opt}} \propto L_{\mathrm{X}}^{1/2}(M_p + M_c)^{1/3}P^{2/3}$. For Cen X-4 we adopt $M_p = 1.4\ M_\odot$, $M_c = 0.23\ M_\odot$ (mass ratio $q = 0.16$), and $P_{\mathrm{orb}} = 0.6290522$ days.

(IV) The NS surface X-ray emission must be removed (if present). It is $\sim$50% of the bolometric X-ray luminosity for Cen X-4.

(V) The inclination should be normalized to that of Cen X-4 using $L_{\mathrm{opt}} \propto \cos(i)$, where $i = 32°\pm^{8°}_{2°}$. We did not correct the figure for this effect because the measure of i is model dependent and the inclination of Cen X-4 within uncertainty is consistent with that of V404 Cyg ($i = 52° \pm 4°$; Shahbaz et al. 1994).

4.2. Energetics

To unambiguously assess whether reprocessing is a valid explanation for the observed correlation, we must take into account that in the reprocessing scenario, the optical reprocessed luminosity is just a small fraction of the X-ray luminosity (a few percent in outburst, less than 2% in quiescence) if the disk is geometrically thin (Shakura & Sunyaev 1973).

We start exploring the outburst data. In the case of the BH system we first subtract the dominating jet contribution in outburst. Moreover, we only account for the X-ray bolometric correction, and not for the accretion disk size. Then we compare the optical luminosity to that in the X-ray. From the power-law fit to the correlation we measure

$L_V/L_X \sim 0.04\%$–0.1% for Cen X-4 and $L_R/L_X \sim$ 0.6%–2.4% for V404 Cyg, two values fully consistent with the reprocessing scenario. Even considering a wider optical–UV range (e.g., not only the R or the V band), the ratio would remain small for both systems and consistent with reprocessing.

On the contrary, during quiescence the X-ray flux of both sources is much fainter. Consequently, in order to properly compare the energetics, we need to consider the contribution of the extra light (e.g., in excess of that coming from the companion) in the whole optical and UV band. For Cen X-4 we used the *Swift* optical–UV and X-ray data (obsid = 0003532019) presented in Bernardini et al. (2013). From the SED we measured a total excess optical–UV luminosity (excluding the *Swift* UVM2 band because it overlaps with others) of $(2.3–3.8) \times 10^{32}$ erg s^{-1}, which we compare with the X-ray luminosity. We here use the 0.01–200 keV luminosity, where we also include the extreme UV and the soft X-ray bands that are expected to produce reprocessing, with the caveat that the real spectral shape below 0.5 keV is not known. We extrapolate the X-ray spectral model, using the 1σ uncertainty on the parameters of the NS atmosphere and the broken power law. For the latter we used $\Gamma = 1.02 \pm 0.1$ and $E_{\mathrm{cutoff}} = 10.4 \pm 1.4$ keV (see Chakrabarty et al. 2014). We estimate $L_{0.01-200\,\mathrm{keV}} = (1.3 - 1.7) \times 10^{33}$ erg s^{-1}. Correspondingly, we get a ratio $L_{\mathrm{opt-UV}}/L_X \sim 18\%$–22% that seems high due to X-ray reprocessing in a geometrically thin disk only. The ratio is higher than that previously reported by Bernardini et al. (2013), who used instead a simple power-law spectra shape (e.g., without an energy cutoff).

For V404 Cyg, unlike Cen X-4, the companion star dominates at all frequencies in the average SED and in particular in the UV band (see Figure 2), so the disk contribution in the optical is likely small (see also Figure 1 in Hynes et al. 2009). Consequently, as we did for outburst data, we measured the excess emission in V404 Cyg in the optical only, and directly from the power-law fit to the correlation, where we only account for the X-ray bolometric correction. We get $L_R^{\min} \sim 1.8 \times 10^{32}$ erg s^{-1} and $L_R^{\max} \sim 1.8 \times 10^{33}$ erg s^{-1} (where $L_R^{\min}$ and $L_R^{\max}$ are the minimum and maximum of the quiescent R-band excess). We estimate the X-ray luminosity using the high and low count rate spectra presented in Bernardini & Cackett (2014), fitting it with a cutoff power law, where $\Gamma = 1.85 \pm 0.15$ and $E_{\mathrm{cutoff}} = 19\pm^{19}_{7}$ keV (Rana et al. 2015). From the extrapolation of the X-ray spectral model we get $L_{0.01-200\,\mathrm{keV}}^{\min} \sim 1.0 \times 10^{33}$ erg s^{-1} and $L_{0.01-200\,\mathrm{keV}}^{\max} \sim 3.1 \times 10^{33}$ erg s^{-1}. Consequently, we measure $L_{\mathrm{opt-UV}}/L_X \sim 18\%$–58%. We notice that this range is very sensitive to the power-law parameters. Taking into account the 3σ uncertainty on it, we get $L_{\mathrm{opt-UV}}/L_X \sim 7\%$–20%.

We conclude that reprocessing in a geometrically thin disk can easily explain the optical–UV excess in outburst for both Cen X-4 and V404 Cyg (once the jet contribution is removed for the latter source). This matches the results of Russell et al. (2006, 2007) for the global population of BH and NS systems. In quiescence, the amount of optical–UV light exceeds that expected from reprocessing in a geometrically thin disk even if we include the contribution from the irradiated surface of the companion. The latter can only reprocess a few percent of the X-ray emission (e.g., ⩽4% in the case of Cen X-4; Bernardini et al. 2013). However, in the case of V404 Cyg, some residual

intrinsic (e.g., not reprocessed) contribution from the disk could still be present, reducing the ratio L_{opt-UV}/L_X. Unfortunately, it is difficult to constrain the exact amount of this residual contribution with the currently available SED. We point out that in quiescence the real structure of the disk is still unknown. If the outer edge of the disk is thicker (e.g., because of the matter that accumulates on the stream impact point), or if the disk is warped, or if the X-ray source is not point-like, and/or the emission originates above the disk plane, like in the so-called "lamp-post" geometry (Nayakshin & Kallman 2001), the maximum amount of reprocessed light would increase and could match the observed ratio. In this respect, we notice that Dubus et al. (1999), using a self-consistent X-ray irradiated accretion disk model, showed that the outer disk of LMXBs can only be irradiated by the central X-ray source if the latter is located above the disk plane or if the disk is warped, or both (because of the self-screening from the inner disk). Moreover, we emphasize that the real spectral shape of both sources below 0.5 keV is not known. For example, the boundary layer of the disk could produce seed photons for reprocessing, and its emission could peak below 0.5 keV. This would further reduce the ratio L_{opt-UV}/L_X.

Campana & Stella (2000) suggested that for NS LMXBs the UV and X-ray emission could be produced at the shock between the matter transferred from the companion and the pulsar relativistic wind under the hypothesis that the NS possesses a weak, rapidly rotating magnetosphere. In this case, accretion down to the NS surface may be halted, and a correlation between the UV and the X-ray power-law flux is expected. However, for Cen X-4 the UV emission is also correlated with the thermal emission (which is changing in tandem with the power-law one), suggesting that matter finally reaches the NS surface (Bernardini et al. 2013).

5. CONCLUSIONS

We have collected for the first time quasi-simultaneous optical (V, R bands) and X-ray luminosity, together with radio to UV SEDs, from outburst to quiescence, for two of the best-studied transient LMXBs: the NS system Cen X-4 and the BH system V404 Cyg.

We found that for Cen X-4 a strong correlation of the form $L_{opt} \propto L_X^{0.44}$ holds over six orders of magnitude in X-ray luminosity. A similar correlation is found for V404 Cyg in outburst during the hard state, where $L_{opt} \propto L_X^{0.56}$, and in quiescence, where $L_{opt} \propto L_X^{0.46}$. However, the optical quiescent data of V404 Cyg are a factor of 4–15 underluminous, based on the extrapolation of the outburst correlation alone, namely, there is a change also in the normalization of the correlation before entering in the quiescent state. Moreover, we found the BH to be optically brighter than the NS at a given X-ray luminosity by a factor of 160–280 in outburst and a factor of about 13–25 in quiescence.

We found from the SEDs of V404 Cyg in outburst that the jet contributes the majority of the optical flux during the hard state, whereas in the soft state the (probably irradiated) disk dominates the optical emission. We identified the main physical mechanisms that make V404 Cyg optically brighter than Cen X-4 for a given X-ray luminosity. Once we consider the bolometric X-ray emission and we account for the fact that the optical emission during the BH outburst hard state is jet dominated, while the jet very likely produces a negligible contribution in the case of the NS (in both outburst and quiescence), that the BH is more massive and has a larger accretion disk, and for Cen X-4 in quiescence we only consider the X-ray emission produced by the power-law spectral component (namely, the emission from the NS surface is subtracted), the two systems lie on the same correlation: a single power law with slope close to 0.5, extending from outburst to quiescence.

We have also shown that for V404 Cyg in outburst (hard state), two mechanisms, the dominant jet and X-ray reprocessing, are responsible for the observed L_X–L_{opt} correlation. During quiescence instead, the contribution of the jet is minimal. This is what probably produces the changes in the normalization and slope of the uncorrected correlation of V404 Cyg. For Cen X-4 in outburst, X-ray irradiation and reprocessing from the disk are very likely the dominating mechanisms in producing the correlation. For both sources in quiescence (in particular for Cen X-4), the ratio between optical–UV and X-ray luminosity is above that expected from reprocessing in a geometrically thin accretion disk. We speculate that the emission from the boundary layer of the disk could peak below 0.5 keV, or that the outer disk could be thicker, the disk could be warped, and/or the irradiating X-ray source could be extended, and/or above the disk plane.

Based on the present study, we suggest that the three main factors, the jet contribution, the accretion disk size (proportional to the orbital period), and the X-ray bolometric correction, could account for the global difference between the optical/X-ray relationship of the population of BH and NS transients. The effects due to the system inclination should also be considered (but were marginal when comparing Cen X-4 and V404 Cyg). The average difference in optical luminosity for the two global populations is a factor of ~20 (Russell et al. 2006), but it is expected to vary from case to case. This can be verified through detailed studies of the other systems.

In this respect, we generate a plot (Figure 4, right panel) where we show a *universal* L_{opt}–$L_{0.5-200\,keV}$ correlation for reprocessing only. The plot is normalized to the parameters of Cen X-4. The jet contribution in the optical band is removed, the primary mass is $1.4 M_\odot$, the mass ratio is $q = 0.16$, the orbital period is $P_{orb} = 0.629$ days (which translates to a disk size $R_{out} \sim 10^{11}$ cm), the X-ray emission from the NS surface is removed, and the orbital inclination is $i = 32°$. We provide details on how to update this figure to include new data (from other sources and from new outbursts of V404 Cyg and Cen X-4).

REFERENCES

Baglio, M. C., D'Avanzo, P., Campana, S., & Covino, S. 2014, A&A, 566, A9

Baglio, M. C., D'Avanzo, P., Muñoz-Darias, T., Breton, R. P., & Campana, S. 2013, A&A, 559, A42

Barthelmy, S. D., D'Ai, A., D'Avanzo, P., et al. 2015a, GCN, 17929

Barthelmy, S. D., Page, K. L., & Palmer, D. M. 2015b, GCN, 18716

Belloni, T. M. 2010, in Lecture Notes in Physics, Vol. 794, ed. T. Belloni (Berlin: Springer), 53

Bernardini, F., & Cackett, E. M. 2014, MNRAS, 439, 2771

Bernardini, F., Cackett, E. M., Brown, E. F., et al. 2013, MNRAS, 436, 2465
Bernardini, F., Russell, D. M., & Lewis, F. 2015, ATel, 7761, 1
Bernardini, F., Russell, D. M., Shaw, A. W., et al. 2016, ApJL, 818, L5
Blair, W. P., Raymond, J. C., Dupree, A. K., et al. 1984, ApJ, 278, 270
Cackett, E. M., Brown, E. F., Degenaar, N., et al. 2013, MNRAS, 433, 1362
Campana, S., & Stella, L. 2000, ApJ, 541, 849
Canizares, C. R., McClintock, J. E., & Grindlay, J. E. 1980, ApJL, 236, L55
Cannizzo, J. K. 1993, ApJ, 419, 318
Cardelli, J. A., Clayton, G. C., & Mathis, J. S. 1989, ApJ, 345, 245
Casares, J., Bonifacio, P., González Hernández, J. I., Molaro, P., & Zoccali, M. 2007, A&A, 470, 1033
Casares, J., & Charles, P. A. 1994, MNRAS, 271, L5
Casares, J., Charles, P. A., Jones, D. H. P., Rutten, R. G. M., & Callanan, P. J. 1991, MNRAS, 250, 712
Casares, J., Charles, P. A., Naylor, T., & Pavlenko, E. P. 1993, MNRAS, 265, 834
Chakrabarty, D., Tomsick, J. A., Grefenstette, B. W., et al. 2014, ApJ, 797, 92
Chevalier, C., Ilovaisky, S. A., van Paradijs, J., Pedersen, H., & van der Klis, M. 1989, A&A, 210, 114
Conner, J. P., Evans, W. D., & Belian, R. D. 1969, ApJL, 157, L157
Corbel, S., Koerding, E., & Kaaret, P. 2008, MNRAS, 389, 1697
Corbel, S., Nowak, M. A., Fender, R. P., Tzioumis, A. K., & Markoff, S. 2003, A&A, 400, 1007
Coriat, M., Corbel, S., Buxton, M. M., et al. 2009, MNRAS, 400, 123
D'Avanzo, P., Campana, S., Casares, J., et al. 2005, A&A, 444, 905
Deller, A. T., Moldon, J., Miller-Jones, J. C. A., et al. 2015, ApJ, 809, 13
Dubus, G., Lasota, J.-P., Hameury, J.-M., & Charles, P. 1999, MNRAS, 303, 139
Frank, J., King, A., & Raine, D. J. 2002, Accretion Power in Astrophysics (3rd ed.; Cambridge: Cambridge Univ. Press)
Gallo, E., Fender, R. P., & Hynes, R. I. 2005, MNRAS, 356, 1017
Gallo, E., Fender, R. P., Miller-Jones, J. C. A., et al. 2006, MNRAS, 370, 1351
Gallo, E., Fender, R. P., & Pooley, G. G. 2003, MNRAS, 344, 60
Gallo, E., Migliari, S., Markoff, S., et al. 2007, ApJ, 670, 600
Gallo, E., Miller, B. P., & Fender, R. 2012, MNRAS, 423, 590
Gallo, E., Miller-Jones, J. C. A., Russell, D. M., et al. 2014, MNRAS, 445, 290
Gandhi, P., Littlefair, S. P., Hardy, L. K., et al. 2016, MNRAS, 459, 554
Gehrz, R. D., Johnson, J., & Harrison, T. 1989a, IAUC, 4816, 3
Gehrz, R. D., Johnson, J., & Harrison, T. 1989b, IAUC, 4786, 1
Gelino, D. M., Gelino, C. R., & Harrison, T. E. 2010, ApJ, 718, 1
González Hernández, J. I., Rebolo, R., Israelian, G., et al. 2005, ApJ, 630, 495
Han, X., & Hjellming, R. M. 1992, ApJ, 400, 304
Hasinger, G., & van der Klis, M. 1989, A&A, 225, 79
Heinz, S., & Sunyaev, R. A. 2003, MNRAS, 343, L59
Hjellming, R. M. 1979, IAUC, 3369, 1
Hjellming, R. M., Rupen, M. P., Mioduszewski, A. J., & Narayan, R. 2000, ATel, 54, 1
Homan, J., Buxton, M., Markoff, S., et al. 2005, ApJ, 624, 295
Hynes, R. I. 2005, ApJ, 623, 1026
Hynes, R. I., Bradley, C. K., Rupen, M., et al. 2009, MNRAS, 399, 2239
Hynes, R. I., Charles, P. A., Casares, J., et al. 2003, MNRAS, 340, 447
Hynes, R. I., Charles, P. A., Garcia, M. R., et al. 2004, ApJL, 611, L125
Hynes, R. I., & Robinson, E. L. 2012, ApJ, 749, 3
Hynes, R. I., Robinson, E. L., & Morales, J. 2015, ATel, 7710, 1
Kaluzienski, L. J., Holt, S. S., & Swank, J. H. 1980, ApJ, 241, 779
Khargharia, J., Froning, C. S., & Robinson, E. L. 2010, ApJ, 716, 1105
Kuulkers, E., in't Zand, J. J. M., & Lasota, J.-P 2009, A&A, 503, 889
Lasota, J.-P. 2001, NewAR, 45, 449
Leibowitz, E. M., Ney, A., Drissen, L., Grandchamps, A., & Moffat, A. F. J. 1991, MNRAS, 250, 385
Lewis, F., Russell, D. M., Jonker, P. G., et al. 2010, A&A, 517, A72
Maitra, D., & Bailyn, C. D. 2008, ApJ, 688, 537
Makino, F. 1989, IAUC, 4782, 1
Markoff, S., Falcke, H., & Fender, R. 2001, A&A, 372, L25
Markoff, S., Nowak, M., Corbel, S., Fender, R., & Falcke, H. 2003, A&A, 397, 645
Markoff, S., Nowak, M. A., & Wilms, J. 2005, ApJ, 635, 1203
Martí, J., Luque-Escamilla, P. L., & García-Hernández, M. T. 2016, A&A, 586, A58
Matsuoka, M., Inoue, H., Koyama, K., et al. 1980, ApJL, 240, L137
Migliari, S., & Fender, R. P. 2006, MNRAS, 366, 79
Migliari, S., Tomsick, J. A., Miller-Jones, J. C. A., et al. 2010, ApJ, 710, 117
Miller-Jones, J. C. A., Jonker, P. G., Dhawan, V., et al. 2009, ApJL, 706, L230
Muno, M. P., & Mauerhan, J. 2006, ApJL, 648, L135
Nayakshin, S., & Kallman, T. R. 2001, ApJ, 546, 406
Nowak, M. A., Wilms, J., & Dove, J. B. 2002, MNRAS, 332, 856
Nowak, M. A., Hanke, M., Trowbridge, S. N., et al. 2011, ApJ, 728, 13
Pavlenko, E. P., Martin, A. C., Casares, J., Charles, P. A., & Ketsaris, N. A. 1996, MNRAS, 281, 1094
Pe'er, A., & Markoff, S. 2012, ApJ, 753, 177
Plotkin, R. M., Gallo, E., Markoff, S., et al. 2015, MNRAS, 446, 4098
Rana, V., Loh, A., Corbel, S., et al. 2015, ApJ, 821, 103
Richter, G. A. 1989, IBVS, 3362, 1
Ritter, H., & Kolb, U. 2003, A&A, 404, 301
Russell, D. M., Fender, R. P., Hynes, R. I., et al. 2006, MNRAS, 371, 1334
Russell, D. M., Fender, R. P., & Jonker, P. G. 2007, MNRAS, 379, 1108
Russell, D. M., Maitra, D., Dunn, R. J. H., & Markoff, S. 2010, MNRAS, 405, 1759
Russell, D. M., Markoff, S., Casella, P., et al. 2013, MNRAS, 429, 815
Rykoff, E. S., Miller, J. M., Steeghs, D., & Torres, M. A. P. 2007, ApJ, 666, 1129
Shahbaz, T., Dhillon, V. S., Marsh, T. R., et al. 2003, MNRAS, 346, 1116
Shahbaz, T., Naylor, T., & Charles, P. A. 1993, MNRAS, 265, 655
Shahbaz, T., Ringwald, F. A., Bunn, J. C., et al. 1994, MNRAS, 271, L10
Shahbaz, T., Russell, D. M., Zurita, C., et al. 2013, MNRAS, 434, 2696
Shahbaz, T., Watson, C. A., & Dhillon, V. S. 2014, MNRAS, 440, 504
Shahbaz, T., Linares, M., Nevado, S. P., et al. 2015, MNRAS, 453, 3461
Shakura, N. I., & Sunyaev, R. A. 1973, A&A, 24, 337
Udalski, A., & Kaluzny, J. 1991, PASP, 103, 198
van Paradijs, J., & McClintock, J. E. 1994, A&A, 290, 133
Wagner, R. M., Bertram, R., Starrfield, S. G., et al. 1991, ApJ, 378, 293
Wagner, R. M., Kreidl, T. J., Howell, S. B., & Starrfield, S. G. 1992, ApJL, 401, L97
Wang, X., & Wang, Z. 2014, ApJ, 788, 184
Xie, F.-G., Yang, Q.-X., & Ma, R. 2014, MNRAS, 442, L110
Zdziarski, A. A., Stawarz, Ł., Pjanka, P., & Sikora, M. 2014, MNRAS, 440, 2238
Zurita, C., Casares, J., Hynes, R. I., et al. 2004, MNRAS, 352, 877
Zurita, C., Casares, J., & Shahbaz, T. 2003, ApJ, 582, 369
Zycki, P. T., Done, C., & Smith, D. A. 1999a, MNRAS, 305, 231
Życki, P. T., Done, C., & Smith, D. A. 1999b, MNRAS, 309, 561